Optimized Source Placement for Multipartite State Distribution in Quantum Networks

Zheng Zhang[1], Qiaolun Zhang[1,*], Jiaheng Xiong[1], Alberto Gatto[1], Raouf Boutaba[2], and Massimo Tornatore[1]
[1]Department of Electronics, Information and Bioengineering, Politecnico di Milano, Milan, Italy
[2]School of Computer Science, University of Waterloo, Waterloo, Canada
[*]Corresponding author: qiaolun.zhang@polimi.it

***Abstract*—The evolution of quantum networks towards distributed quantum computing and sensing necessitates the efficient distribution of multipartite entangled states among multiple users. However, most existing entanglement routing studies primarily focus on efficient entanglement distribution and typically assume that quantum sources are either fixed or available on all network edges. Due to the scarcity and high cost of quantum sources, some prior studies have focused on optimized source placement strategies, but these existing studies are confined to bipartite state distributions. Consequently, how to jointly optimize quantum source placement and entanglement routing for efficient multipartite state distribution under realistic resource constraints remains an open problem. In this work, we propose an Optimized source Placement and Reactive entanglement Routing (OP-RR) framework to maximize the multipartite state distribution rate given a limited amount of quantum sources. Numerical results on a grid and on the Tokyo topology demonstrate that OP-RR consistently outperforms baseline algorithms with non-optimized source placement, achieving an improvement of up to $16.7\times$ in the multipartite distribution rate, while maintaining robustness under varying operation probabilities and scalability as the size of multipartite states increases.**

***Index Terms*—Quantum source placement, multipartite state, entanglement distribution**

I. Introduction

The rapid advancement of quantum technologies calls for novel algorithmic solutions to effectively allocate quantum-network resources for entanglement distribution to facilitate emerging applications, such as secure communications [1]–[3] and distributed sensing [4], [5]. While traditional entanglement distribution typically relies on bipartite entangled states shared between two nodes, several emerging applications, such as distributed quantum computation [6], can benefit from multipartite states shared among multiple nodes to enable coordinated quantum tasks. Either bipartite or multipartite, entangled states rely on quantum sources that probabilistically generate entanglement links across a network. Recent works have proposed various *Entanglement Routing* (ER) schemes to improve the efficiency of entanglement distribution [7], [8]. However, most existing studies assume that the location of quantum sources is fixed and that quantum sources are available at all edges, which is unrealistic given their limited availability [1] and high cost [9]. To address the problem of scarcity of quantum sources, previous works investigated optimized source placement for bipartite state distribution [10], [11]. However, these studies do not consider *multipartite state distribution*, which requires more complicated procedures. Specifically, as shown in Fig. 1a for a case of three nodes, multipartite state distribution not only requires *entanglement swapping* to generate long-distance bipartite states, but it also requires *entanglement fusion* to generate a multipartite state [12]. Therefore, a key open challenge is to effectively coordinate optimized quantum source deployment and ER for efficient multipartite state distribution.

To the best of our knowledge, this work is the first to address optimized quantum source placement for multipartite state distribution. We investigate the impact of proactive vs. reactive ER on the resulting *Distribution Rate* (DR), defined as the average number of multipartite states distributed per time slot under constrained quantum source resources. We propose a new algorithm for **O**ptimized source **P**lacement and **R**eactive entanglement **R**outing (OP-RR) aimed at maximizing DR. Extensive numerical simulations on two representative topologies, a 4×4 grid network and a 12-node Tokyo network [13], demonstrate that OP-RR achieves the highest distribution rate (up to $16.7\times$ higher compared to baseline source deployments), remains robust under varying operation probabilities, and scales effectively as the size of multipartite states increases.

II. Optimized Source Placement for Multipartite State Distribution

A. Network Model and Problem Statement

We consider a quantum network modeled as an undirected graph $G = (V, E)$. Nodes V represent quantum nodes. A request R is represented by a subset of nodes $S \subseteq V$, referred to as user nodes, requiring to generate multipartite states among $N = |S|$ users. Each $e \in E$ edge is implemented with quantum channels realized over optical fibers. As illustrated in Fig. 1a, each quantum source is directly connected to two quantum nodes with a quantum channel [10]. The quantum source generates a pair of qubits that are stored at quantum nodes, thereby establishing an entanglement link. In this configuration, each quantum source is directly connected to the two quantum nodes with a dedicated quantum channel [10]. For a fiber of length L km with attenuation coefficient 0.2 dB/km, the probability of successfully creating an entanglement link is modeled as: $p_e = p_{\text{op}}(1 - p_{\text{loss}})$ [12], where $p_{\text{op}} \in [0, 1]$ denotes the operation probability capturing imperfections such as photon emission, and $p_{\text{loss}} = 10^{-0.2L/10}$

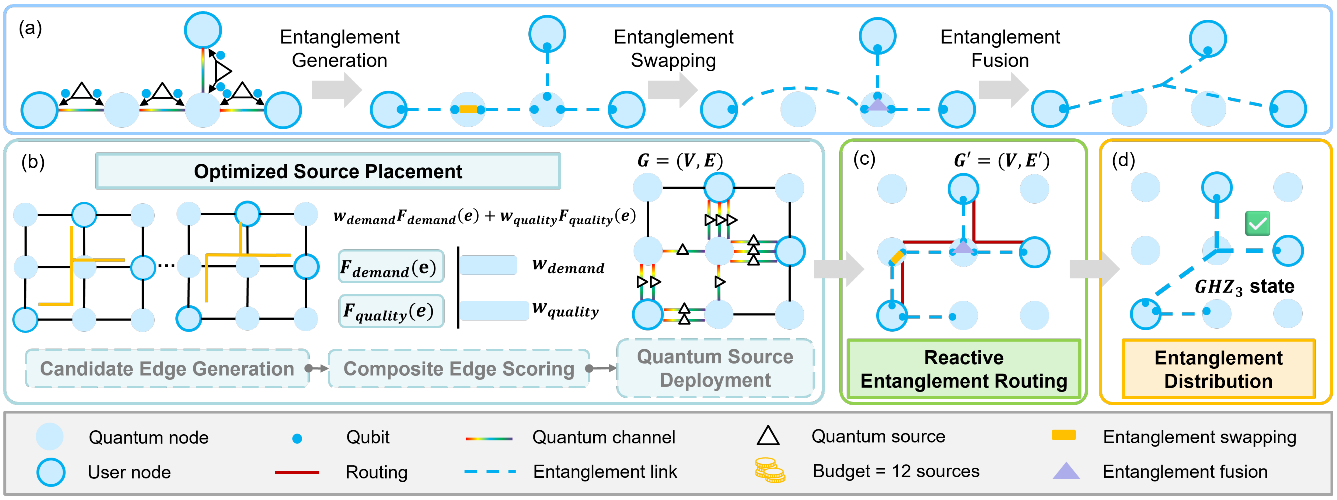

Fig. 1. Optimized quantum-source placement and reactive entanglement routing.

denotes the loss probability due to fiber attenuation. The network operation is modeled in discrete time slots of duration T_{slot}. During each slot, all quantum sources attempt to generate entanglement links simultaneously. Memory decoherence for the entanglement link is represented by a cut-off time T_c as in [7], corresponding to $Q_c = \lfloor T_c/T_{\text{slot}} \rfloor$ time slot.

The optimized source placement problem for multipartite state distribution can be stated as follows: **Given** a quantum network topology, a request for multipartite state distribution (as commonly considered in prior work [12], [14]), and a budget of deployable quantum sources, **decide** how many quantum sources to deploy on each edge, and how to determine entanglement routing and perform entanglement swapping and fusion among user nodes, **constrained** by the limited quantum memories at each node, the finite cut-off time, and the budget that restricts the total number of quantum sources that can be deployed. **The objective** is to maximize DR of N-qubit Greenberger–Horne–Zeilinger (GHZ_N) states [15].

B. Optimized Quantum-Source Placement

Under the request and resource constraints defined above, quantum-source placement plays a key role in enabling efficient ER. Accordingly, we develop an optimized quantum-source placement (OP) strategy that allocates a limited number of quantum sources to network edges. OP follows the three-stage workflow in Fig. 1b, consisting of candidate edge generation, composite edge scoring, and quantum source deployment as follows.

a) Candidate Edge Generation: Firstly, OP identifies a set of candidate edges frequently involved in feasible routes among the user nodes in R. K Steiner trees $\{T_1, T_2, \cdots, T_K\}$ are computed to connect user nodes with minimum total length [12], forming an edge set $E_{\text{tree}} = \bigcup_{k=1}^{K} E(T_k)$. Meanwhile, k_{path} shortest paths are extracted for each user pair, and the edge set E_{path} is combined with E_{tree} to generate the candidate edge set $E_{cand} = E_{tree} \cup E_{path}$, shown as yellow lines in the left part of Fig. 1b.

b) Composite Edge Scoring: Then, each candidate edge in E_{cand} is evaluated by a composite score that reflects both topological significance in connecting user nodes of R and its physical-layer performance:

$$\text{Score(e)} = w_{\text{demand}} F_{\text{demand}}(e) + w_{\text{quality}} F_{\text{quality}}(e) \quad (1)$$

where F_{demand} quantifies how frequently the edge appears across the K Steiner trees and user-pair shortest paths, and $F_{quality}$ corresponds to entanglement success probability p_e. In this work, equal weights are adopted for the two components. Corresponding to the middle part in Fig. 1b, OP provides a quantitative basis for effective source allocation by combining these weighted factors.

c) Quantum Source Deployment: Finally, as illustrated in the right part of Fig. 1b, OP determines the number of quantum sources x_e to be deployed on each candidate edge under a total budget B, which is modeled as a multiple-choice knapsack problem. For each edge, the gain is $G_e(x_e) = x_e \cdot \text{Score}(e)$. The global objective is to maximize the total gain over all candidate edges, subject to the total budget B, cost per quantum source C_s, and per-edge source cap $x_{\max}$, shown as:

$$\begin{aligned} &\max_{\{x_e\}} \sum_{e \in E_{\text{cand}}} G_e(x_e) \\ \text{s.t.} \quad &\sum_{e} x_e \le \lfloor B/\text{C}_\text{s} \rfloor, 0 \le x_e \le x_{\max} \end{aligned} \quad (2)$$

This discrete optimization can be efficiently solved through a grouped dynamic programming (DP) approach [16], which incrementally explores all edges under increasing budget values. For each edge e_i and budget $b \le \lfloor B/\text{C}_\text{s} \rfloor$, the DP state $\text{dp}[i][b]$ stores the best achievable objective using the first i edges. The state transition is defined as

$$\text{dp}[i][b] = \max_{0 \le x \le \min(x_{\max}, b)} \{\text{dp}[i-1][b-x] + G_{e_i}(x)\} \quad (3)$$

As a result, the DP produces a budget-feasible and non-uniform source placement to support the efficient entanglement routing by prioritizing edges with higher composite scores.

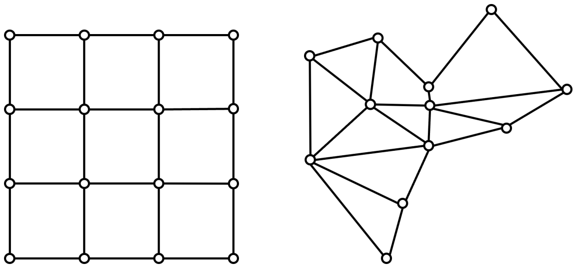

(a) (b)

Fig. 2. Simulation topology (a) grid topology and (b) Tokyo topology.

C. Entanglement Routing for Multipartite Distribution

After running OP to determine the quantum source placement, our proposed approach for multipartite state distribution performs entanglement routing (ER) across successive time slots. In each time slot, every source attempts entanglement generation with probability p_e, updating the subgraph $G' = (V, E')$ in Fig. 1c, where E' is the set of successfully established entanglement links. The routing objective is to distribute a multipartite state connecting all user nodes, which is ultimately achieved through entanglement fusion after extending bipartite states via entanglement swapping.

To achieve this, two ER approaches are considered. Proactive routing (PR) determines fixed, central-node-based routing paths in advance based on the network topology, **before** entanglement links are generated, and applies the same routes in all time slots. In contrast, reactive routing (RR) [12], [17] dynamically constructs a Steiner tree in each time slot according to the currently available entanglement links **after** entanglement generation. Without the constraint of using a central node, the Steiner tree connects all user nodes utilizing the minimum number of entanglement links. As shown in Fig. 1c, a GHZ_N state is formed via entanglement swapping and fusion on the selected tree. We assumed error-free entanglement swapping and fusion as [12] to perform a preliminary study for the network-level optimization. Nonetheless, our solution can be extended to the case of probabilistic operations, which will be performed as an extended version of this paper. Fig. 1d shows how the combinations of quantum source placement optimization and reactive entanglement routing (i.e, the OP-RR algorithm) can successfully distribute a GHZ_N state over established entanglement links.

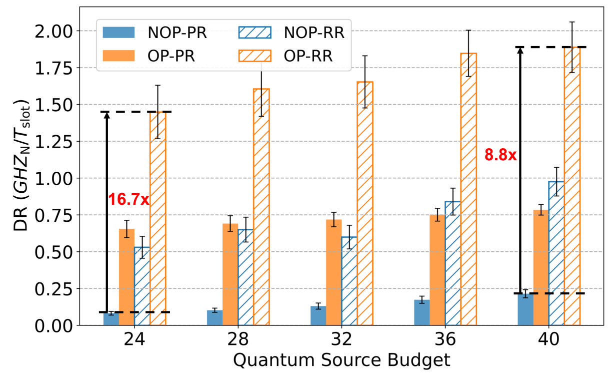

(a)

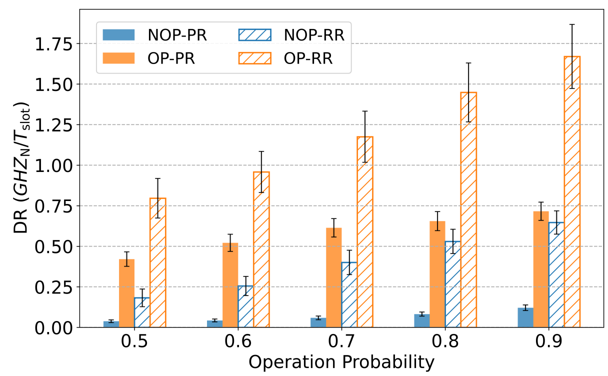

(b)

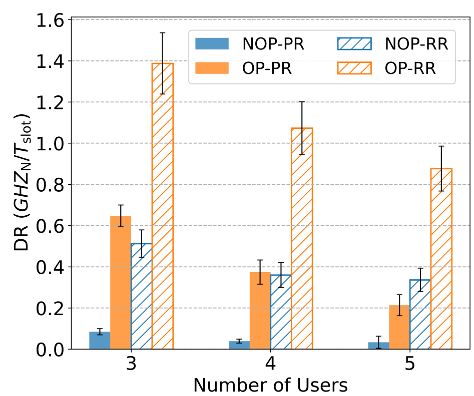

(c)

Fig. 3. Distribution rate (GHZ_N/T_{slot}) vs. (a) quantum source budget, (b) operation probability, and (c) number of users in 4×4 grid topology.

III. Simulation Setup and Results

We evaluate the proposed OP-RR algorithm against three baselines: NOP-PR and NOP-RR (non-optimized source placement with proactive and reactive routing, respectively) and OP-PR (optimized placement with proactive routing). OP follows the algorithm in Sec. II-B. In contrast, NOP distributes quantum sources as uniformly as possible; when B is insufficient for an equal number of quantum sources to all edges, sources are assigned to edges sequentially in ascending edge-index order until the budget is exhausted.

By default, we set $p_{op} = 0.8$, $x_{max} = 5$, $|S| = 3$, and $Q_c = 1$ [12], where $Q_c = 1$ means entanglement links must be consumed within the same time slot they are generated. The cost of each quantum source is normalized to $C_s = 1$, so that the budget B represents the total number of available quantum sources. As shown in Fig. 2, experiments are conducted on a 4×4 grid topology with a uniform link length of 10 km and a 12-node, 21-link Tokyo topology [13] with link lengths ranging from 2.6 to 12.0 km. For the experiments in Figs. 3b-3c, the quantum source budget is fixed to $B = 24$, equal to the number of edges in the grid topology. Similarly, the budget in Figs. 4b-4c in Tokyo topology is fixed to $B = 21$. Each bar represents the average of 100 simulation runs, where each run is initialized with a randomly sampled request and terminates

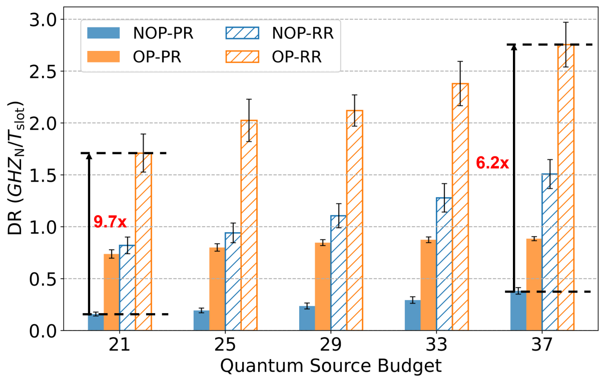

(a)

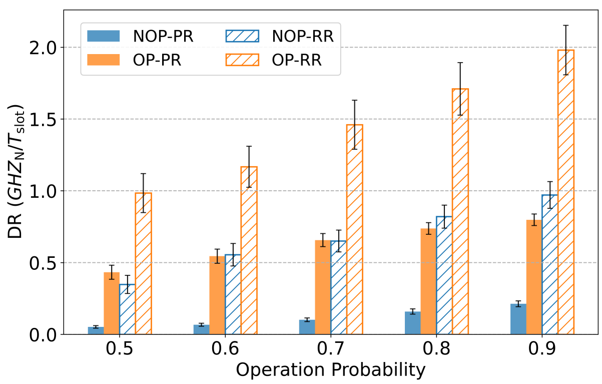

(b)

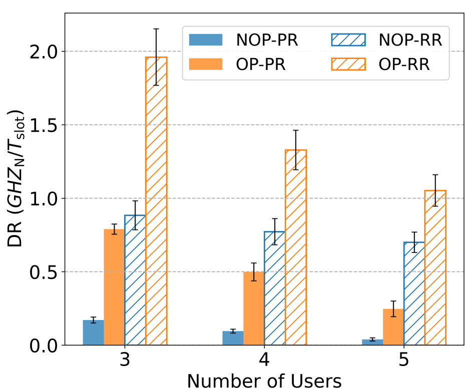

(c)

Fig. 4. Distribution rate (GHZ_N/T_{slot}) vs. (a) quantum source budget, (b) operation probability, and (c) number of users in 12-node Tokyo topology.

after 80 time slots. Error bars denote 95% confidence intervals over 100 independent runs.

Figs. 3a–3c analyze the DR dependency on different parameters in the grid topology. As shown in Fig. 3a, OP-RR consistently achieves the highest DR, achieving up to 16.7$\times$ improvement over NOP-PR under limited budget. This gain results from OP-based approaches prioritizing topologically critical and high-quality edges. As the budget increases, this gain gradually decreases to 8.8$\times$, since both OP-based and NOP-based approaches can eventually cover most important edges, and hence generate enough entanglement links for multipartite state distribution. In Fig. 3b, when the operation probability p_{op} increases DR improves across all approaches because higher p_{op} enhances the likelihood of successful entanglement generation. However, OP-RR remains superior across the full range of p_{op}. In Fig. 3c, as the number of users $|S|$ grows, DR decreases across all approaches because multipartite state generation requires more simultaneous entanglement links. Nevertheless, OP-RR sustains the highest DR, indicating its robustness in supporting larger user groups. Specifically, OP-RR exhibits slightly higher variance, as NOP and PR rely on uniform source distribution and fixed routing decisions, which reduce sensitivity to instantaneous entanglement generation.

Figs. 4a–4c report the results on the larger Tokyo topology. The trends observed on the grid topology persist, while DR values of all approaches become even larger, as Tokyo topology is more densely connected and has shorter average link length with 7.85 km, offering richer path diversity and lower p_{loss}. In Fig. 4a, OP-RR achieves the highest DR under all budgets with up to a 9.7$\times$ improvement over NOP-PR, which confirms the scalability of optimized source placement in irregular topology. Similarly, when p_{op} increases in Fig. 4b, OP-RR consistently outperforms all baselines, demonstrating robust adaptability to probabilistic entanglement generation. Fig. 4c shows that OP-RR maintains efficient GHZ distribution even as the number of user nodes expands.

IV. Conclusion

In this study, we propose an OP-RR algorithm for multipartite state distribution, leveraging optimized source placement (OP) and reactive entanglement routing (RR) under limited quantum sources. We performed extensive evaluations comparing OP-RR against three baselines (NOP-PR, NOP-RR, and OP-PR) on a grid and Tokyo network topology. Results demonstrated that OP-RR consistently achieves the highest distribution rate, up to a 16.7$\times$ improvement. Furthermore, the proposed solution exhibits strong robustness under varying entanglement operation probabilities and scales effectively as the number of user nodes increases.

Acknowledgment

This work was supported in part by funding from the Innovation for Defence Excellence and Security (IDEaS) program from the Canadian Department of National Defence (DND).

References

[1] S. Wehner, D. Elkouss, and R. Hanson, "Quantum internet: A vision for the road ahead," *Science*, vol. 362, no. 6412, p. eaam9288, 2018.

[2] Q. Zhang, O. Ayoub, A. Gatto, J. Wu, F. Musumeci, and M. Tornatore, "Routing, channel, key-rate, and time-slot assignment for qkd in optical networks," *IEEE Transactions on Network and Service Management*, vol. 21, no. 1, pp. 148–160, 2023.

[3] J. Li, P. Zheng, Z. Li, Y. Yang, N. Yu, Q. Sun, and J. Lu, "Decentralized key management and service in quantum key distribution networks: An experimental implementation," *IEEE Journal on Selected Areas in Communications*, vol. 43, no. 8, pp. 2782–2797, 2025.

[4] D.-H. Kim, S. Hong, Y.-S. Kim, K. Oh, S.-Y. Lee, C. Lee, and H.-T. Lim, "Distributed quantum sensing with multimode n 00 n states," *Physical review letters*, vol. 135, no. 5, p. 050802, 2025.

[5] J. Bate, A. Hamann, M. Canteri, A. Winkler, Z. X. Koong, V. Krutyanskiy, W. Dür, and B. P. Lanyon, "Experimental distributed quantum sensing in a noisy environment," *Physical Review Letters*, vol. 135, no. 22, p. 220801, 2025.

[6] S. DiAdamo, M. Ghibaudi, and J. Cruise, "Distributed quantum computing and network control for accelerated vqe," *IEEE Transactions on Quantum Engineering*, vol. 2, pp. 1–21, 2021.

[7] J. Xiong, Q. Zhang, A. Gatto, F. Musumeci, R. Boutaba, and M. Tornatore, "Adaptive entanglement routing for quantum networks with cutoff," in *2023 19th International Conference on Network and Service Management (CNSM)*. IEEE, 2023, pp. 1–5.

[8] Q. Zhang, N. Di Cicco, M. Ibrahimi, R. C. Almeida, A. Gatto, R. Boutaba, and M. Tornatore, "Link configuration for fidelity-constrained entanglement routing in quantum networks," in *IEEE Conference on Computer Communications*. IEEE, 2025, pp. 1–10.

[9] "Thorlabs — thorlabs.com," https://www.thorlabs.com/correlated-photon-pair-sources?tabName=Overview, [Accessed 07-01-2026].

[10] Q. Zhu, Y. Zhao, H. Xu, L. Huang, and C. Qiao, "Beyond entanglement routing: Source assignment and all-optical switching-based distribution," *IEEE/ACM Transactions on Networking*, 2024.

[11] S. Xu, Y. Zhao, L. Huang, and C. Qiao, "Routing and photon source provisioning in quantum key distribution networks," in *IEEE INFOCOM 2024-IEEE Conference on Computer Communications*. IEEE, 2024, pp. 1411–1420.

[12] E. Sutcliffe and A. Beghelli, "Multiuser entanglement distribution in quantum networks using multipath routing," *IEEE Transactions on Quantum Engineering*, vol. 4, pp. 1–15, 2023.

[13] T. Tachibana, Y. Hirota, K. Suzuki, T. Tsuritani, and H. Hasegawa, "Metropolitan area network model design using regional railways information for beyond 5g research," *IEICE Transactions on Communications*, vol. 106, no. 4, pp. 296–306, 2023.

[14] E. Sutcliffe, M. J. Hoban, and A. Beghelli, "Multi-user entanglement routing for quantum mesh networks," in *Optical Fiber Communication Conference*. Optica Publishing Group, 2023, pp. W4K–2.

[15] D. M. Greenberger, M. A. Horne, and A. Zeilinger, *Going Beyond Bell's Theorem*. Dordrecht: Springer Netherlands, 1989, pp. 69–72. [Online]. Available: https://doi.org/10.1007/978-94-017-0849-4_10

[16] D. Pisinger, "Where are the hard knapsack problems?" *Computers & Operations Research*, vol. 32, no. 9, pp. 2271–2284, 2005.

[17] M. Pant, H. Krovi, D. Towsley, L. Tassiulas, L. Jiang, P. Basu, D. Englund, and S. Guha, "Routing entanglement in the quantum internet," *npj Quantum Information*, vol. 5, no. 1, p. 25, 2019.